Aalto University

Zeng, Weijun; Tappura, Kirsi; Kamada, Masahiro; Laitinen, Antti; Seppä, Heikki; Hakonen, Pertti

Second spectrum of 1 / f noise due to mobility fluctuations : Simulations vs experiments in suspended graphene

Please cite the original version:
Zeng, W., Tappura, K., Kamada, M., Laitinen, A., Seppä, H., & Hakonen, P. (2023). Second spectrum of 1 / f noise due to mobility fluctuations : Simulations vs experiments in suspended graphene. *Applied Physics Letters*, *123*(1), 1-6. Article 013509. https://doi.org/10.1063/5.0153467

Second spectrum of $1/f$ noise due to mobility fluctuations: Simulations vs experiments in suspended graphene

Weijun Zeng ; Kirsi Tappura ; Masahiro Kamada; Antti Laitinen ; Heikki Seppä ; Pertti Hakonen

Check for updates

CrossMark

View Online

Export Citation

Second spectrum of $1/f$ noise due to mobility fluctuations: Simulations vs experiments in suspended graphene

View Online   Export Citation   CrossMark

Weijun Zeng,[1,2] (iD) Kirsi Tappura,[3,4] (iD) Masahiro Kamada,[1] Antti Laitinen,[1] (iD) Heikki Seppä,[3,4] (iD) and Pertti Hakonen[1,2,a)] (iD)

AFFILIATIONS

[1]Low Temperature Laboratory, Department of Applied Physics, Aalto University School of Science, P.O. Box 15100, 00076 Aalto, Finland
[2]QTF Centre of Excellence, Department of Applied Physics, Aalto University School of Science, P.O. Box 15100, 00076 Aalto, Finland
[3]Microelectronics and Quantum Technology, VTT Technical Research Centre of Finland Ltd., P.O. Box 1000, 02044 VTT, Finland
[4]Microelectronics and Quantum Technology, VTT Technical Research Centre of Finland Ltd., QTF Centre of Excellence, P.O. Box 1000, 02044 VTT, Finland

Note: This paper is part of the APL Special Collection on Electronic Noise: From Advanced Materials to Quantum Technologies.
[a)]Author to whom correspondence should be addressed: pertti.hakonen@aalto.fi

ABSTRACT

Mobility fluctuations have been observed to influence $1/f$ noise in mesoscopic two-dimensional conductors in recent experiments. If such mobility noise can be assigned to clustering/declustering of defects/impurities, the second spectrum should also display $1/f$ character. In this work, we investigate the second spectrum of noise due to mobile impurities on a two-dimensional lattice both using kinetic Monte Carlo simulations (periodic boundary conditions either in one or two directions) and experiments on suspended graphene in Corbino geometry. The simulations indicate $1/f^\delta$ behavior with $\delta \simeq 0.8 \pm 0.15$ for the second spectrum of noise, while the experiments on suspended graphene yield an exponent $\delta \simeq 0.7 \pm 0.3$, independent of the amount of adsorbed atoms.

In quantum devices and semiconducting heterostructures, $1/f$ noise is typically modeled using a collection of two-level systems (TLS) or trap states,[1–3] which have also been found very important for the loss of coherence in superconducting devices working at microwave frequencies.[4,5] A large collection of such states, having broadly distributed tunneling parameters, facilitates a wideband of $1/f^\gamma$ noise with $\gamma \simeq 1$. Such modeling of low frequency noise has been very successful, e.g., in field-effect transistors.[3] The resistance fluctuations in metallic conductors are determined foremost by fluctuations in charge carrier mobility.[6] Mobility variation can arise due to impurity states with a fluctuating scattering cross section or lattice scattering induced by phonons.[7] At low temperatures, universal conductance fluctuations caused by electron interference in disordered material become modified by defect motion leading to noise.[8,9] Furthermore, there are also $1/f^\gamma$ models based on mobile impurities and their agglomeration.[10–16]

The origin of $1/f$ noise in graphene is complex, in particular, near the charge neutrality point (Dirac point).[17,18] It is argued to arise from an interplay of charge traps, atomic defects, short and long range scattering, as well as charge puddles. Various models have been proposed and qualitative agreement with the data has been reached.[19–25] In many graphene devices, even correlations between charge traps and mobility noise have been found,[26,27] which is also common in regular metallic and semiconducting devices.[1,7,28] Suspended clean graphene removes many of these noise sources and the fundamental elements can be addressed in a non-disturbed form.

Direct evidence has recently been obtained for the role of mobility fluctuations in electrical transport in 2D.[29,30] For these findings, we have proposed a model of $1/f$ noise based on clustering/declustering of impurities and defects,[30,31] which provides intrinsic correlations without any assumptions on the distribution of tunneling or scattering parameters. Long-time memory is naturally encompassed due to the countless number of available reconfigurations among the ensemble of mobile impurities. This authentic $1/f$ noise may become overshadowed by other noise processes present in the actual investigated device,

e.g., several single random fluctuators.[32,33] However, under favorable conditions, the noise due to interacting mobile impurities may become observable. In mesoscopic systems, this noise is stationary with a $1/f$ spectrum with upper and lower cutoff frequencies. Hence, the noise of such noise, the second spectrum $\mathcal{S}_2(f_2, f)$ displays $1/f_2^\delta$ dependence with $\delta = 1$. Colored second spectrum has turned out to be an important tool in studies of interacting TLSs and non-Gaussian fluctuations as discussed, e.g., in Refs. 34–44

In the present work, we address the second spectrum of the noise in both experimental and theoretical model systems where the clustering/declustering of defects or impurities plays an important role. We discuss first the results of kinetic Monte Carlo (kMC) simulations of small 2D systems of 2500 lattice sites, both an infinite box and a Corbino disk, i.e., using periodic boundary conditions in both x and y or only x directions, respectively.[45] We will compare simulations with experimental results of a suspended graphene Corbino disk at 4 and 15 K, measured under current-annealed conditions[31,46] as well as with adsorbed neon. The simulated second spectrum displays $1/f^\delta$ behavior with $\delta \simeq 0.8 \pm 0.15$. In the experiments, $\delta \simeq 0.7 \pm 0.3$. We find lognormal and normal distributions, respectively, for noise magnitudes and exponents, derived from extensive time series of noise spectra (∼1000 spectra). Similar non-Gaussian behavior is also found in simulations.

According to the model discussed in Refs. 30 and 31, the power spectral density of $1/f$ fluctuations can be related to the fluctuations in μ_m, which describes the mobility limited by mobile impurities alone; the corresponding conductivity is $\sigma_m = en\mu_m$, where n is the density of charge carriers. According to this model, the spectral density of $1/f$ noise $S_m(f)$ is given by (here $\langle \Delta\sigma_m^2 \rangle$ refers to variance),

$$S_m(f) = \frac{\langle \Delta\sigma_m^2 \rangle}{\langle \sigma_m \rangle^2} = \frac{\langle \Delta\mu_m^2 \rangle}{\mu_m^2} = \mathbf{s}_m \frac{1}{f}, \qquad (1)$$

where $\mathbf{s}_m$ can be viewed as an experimentally determined parameter which, in theory, has a fixed mean value $\langle \mathbf{s}_m \rangle = $ const. (provided that the number of impurities is fixed[30]). This formulation differs from Hooge's[6,47] law, which states that the $1/f$ noise due to mobility fluctuations is inversely proportional to the total number of charge carriers N_e. Thus, this approach parallels those of Refs. 9 and 48.

In a bounded, isolated system, where noise is governed by a finite number of configurations of the hopping scatterers, the $1/f$ noise spectrum does not extend to zero frequency and the (total) noise spectrum can be written in the following form:[30]

$$S_m(f) = \mathbf{s}_m^* \frac{f_d}{f^2 + ff_u + f_u f_d} \qquad (2)$$

with $\mathbf{s}_m^* = \mathbf{s}_m \times (f_u/f_d)$. Here, the upper cutoff f_u is given by the hopping frequency and the lower cutoff f_d reflects the stationarity of the small system. For the spectrum in Eq. (2) with genuine $1/f$ correlations, the low frequency values of $1/f$ reflect the deviation of averaged current fluctuations $\frac{1}{T}\int_0^T (I(t) - \langle I(t) \rangle) dt$ from the long-time mean of current $\langle I(t) \rangle$. These averages preserve the $1/f$ noise nature and, thus, the second spectrum should also display $1/f$ character.

Apart from mobile impurities, the conductance is influenced by immobile impurity scattering, either due to short-ranged scatterers or Coulomb impurities, resulting in a mobility μ_i; here, we assume sufficiently low temperatures so that electron–phonon scattering can be

neglected. The graphene conductivity is then $\frac{1}{\sigma_g} = \frac{1}{ne}\left(\frac{1}{\mu_i} + \frac{1}{\mu_m}\right)$, in accordance with the Mathiessen rule of adding scattering rates. Consequently, the conductance fluctuation of graphene can be written as

$$S_g(f) = \frac{\langle \Delta\sigma_g^2 \rangle}{\sigma_g^2} = \left(\frac{\mu_g}{\mu_m}\right)^2 \mathbf{s}_m^* \frac{f_d}{f^2 + ff_u + f_u f_d} \simeq \left(\frac{\mu_g}{\mu_m}\right)^2 \mathbf{s}_m \frac{1}{f}, \qquad (3)$$

where $\frac{1}{\sigma_g} = \frac{1}{ne}\frac{1}{\mu_g}$ and the last approximate equality is valid when $f_d \ll f \ll f_u$. The actual emerging noise, thus, depends on the significance of μ_m with respect to the total graphene mobility μ_g. If there are only a few mobile impurities, $\mu_m \gg \mu_i$ and the $1/f$ noise becomes small.

Kinetic Monte Carlo simulation[49,50] is a powerful tool to investigate particle dynamics on a 2D lattice in the presence of particle–particle interactions. Our simulated system consists of a 50×50 square lattice (2500 sites) with about 25 impurities (density of 1%), initially randomly positioned on the lattice sites. We impose periodic boundary conditions either in both x and y directions ("infinite box") or only in x direction (strip of cylinder emulating a "Corbino disk"). All lattice sites are taken as equivalent for impurity atoms, i.e., we neglect the influence of strain deformations induced by the impurities in the graphene membrane. We also neglect possible repulsion of the impurities at short distances and simply allow the particles to occupy the nearest unoccupied neighbor sites without overlapping. For details of the simulation, we refer to Ref. 31.

A defect can hop to any of its eight adjacent sites on a square lattice by thermally activated hopping. The average hopping rate without any change or with an increase (decrease in system energy) in the coordination number is given by $r = f_A \exp\left(\frac{-E_d}{k_B T}\right)$, where f_A is the attempt frequency, E_d is the activation energy for the hopping path, and T is the temperature. If the coordination number decreases (e.g., a particle dissociates from a cluster), the relevant interaction energy change ΔE has to be included.[31] Thus, there is an increase in the activation energy for dissociation but not for agglomeration. In our present simulations, we have set $f_A = 1$, $E_d = 4$ (for real parameter values, see Refs. 51–54) and $k_B T = 1.2$ or $k_B T = 2$. The most important parameter is the ratio $\frac{-(E_d + \Delta E)}{k_B T}$, which governs the hopping rate with coordination with edges, immobile, and other mobile defects. In fact, the hopping barrier for entering a cluster could be different from free hopping. However, what matters for the clustering dynamics is the difference between the in- and out-hopping barriers which can be specified using one parameter ΔE.[55] Noise generation by clustering/declustering of impurities can work also at room temperature.

To calculate noise spectra, one needs resistance values at preset time instances separated by Δt, which we determine using continuum modeling. We set the conductivity of impurity sites 10^{-5} times smaller than the background conductivity. We employed finite element method[56] for resistance evaluation, which is computationally quite demanding.[31] In order to save computational resources, the resistance values were calculated only at sampling times needed for the intended frequency range (up to $1/2\Delta t$) of the first spectrum $S_R(f)$. Second spectra $\mathcal{S}_2(f_2, f)$ were calculated from a time series of integrated noise $A_j(t_j) = \int_{f_0}^{f_1} S_R(f, t_j) df$, where f_0 and f_1 were chosen to reside mainly between the corner frequencies f_d and f_u, producing effectively a $1/f^{0.8}$ type characteristics in the second spectra. When working with spectral
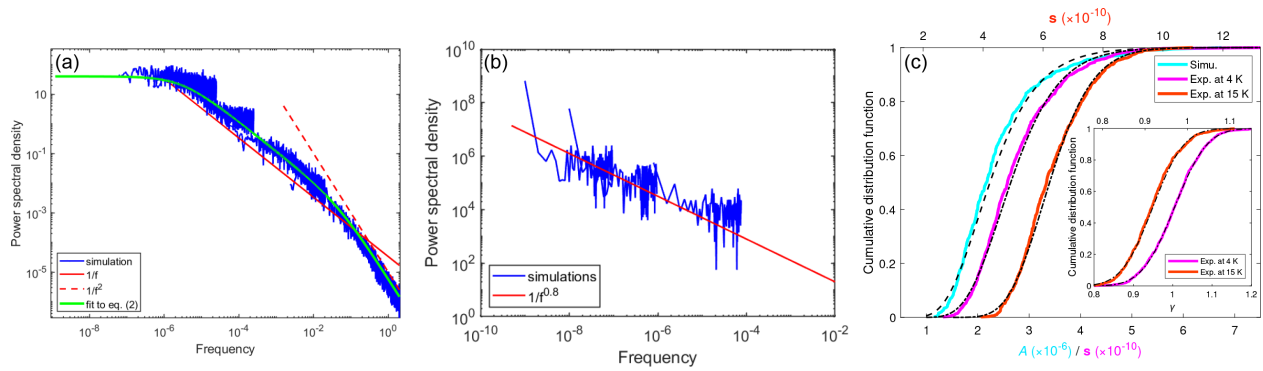
FIG. 1. (a) Simulated resistance noise power spectrum $S_R(f)$ of an infinite box obtained for $k_B T = 1.2$. Four different time steps were employed in resistance sampling to cover the whole range of frequencies. (b) Power spectral density of second spectrum $S_2(f_2) \times 10^{10}$ of the scaled resistance noise integral $A(t_j) = \int_{f_0}^{f_1} S_R(f, t_j)df$ calculated for infinite box using three different time steps T_{step} between the simulated noise power spectra ($t_j = jT_{step}$). Integration limits f_0 and f_1 were chosen within the $1/f$ range from $f_d = 3 \, \mu Hz$ to $f_u = 0.05 \, Hz$ determined from Fig. 1(a). (c) Cumulative distribution function for the scaled resistance noise integral data $A(t_j)$ of Corbino geometry simulated for $k_B T = 2$ as well as for the noise magnitude **s** of the noise spectra measured near the Dirac point at $V_g = -1.20 \, V$ ($n = -1.22 \times 10^{10} \, cm^{-2}$) at 4 K (magenta trace and bottom scale, the data illustrated in Fig. 3) and 15 K (red trace and top scale). The dashed and dashed–dotted curves illustrate lognormal fits to the data. The inset displays cumulative distribution function of noise exponent γ of 4 and 15 K data with normal distribution fits.

frequencies $f_d < f < f_u$, the calculated $\mathcal{S}_2(f_2, f)$ was found independent of f and, consequently, we denote these second spectra as $S_2(f_2)$.

Figure 1(a) displays the power spectral density of resistance fluctuations obtained for simulations performed for temperature $k_B T = 1.2$, with strong resistance at the scattering sites; practically, the same behavior is obtained by setting large conductance at the impurity sites. The shape of the power spectral density agrees well with the form in Eq. (2), which is depicted in Fig. 1(a) as the solid green curve. There is clearly a tendency toward a plateau at the lowest frequencies below $f_d \simeq 1 \, \mu Hz$ and a crossover to $1/f^2$ spectrum above the hopping frequency corresponding here to $f_u \simeq 0.05 \, Hz$. The step-like behavior of the calculated noise spectra arises due to computational resource limitations, i.e., the sampling frequency near the steps falls below the Nyquist frequency of the data and, thus, the spectra are distorted by aliasing.

In order to investigate the variation of noise magnitude in time, we have calculated a sequence of noise spectra in the range of frequencies displayed in Fig. 1(a). The time step T_{step} between the spectra sets the upper frequency $f_2^{max} = 1/2T_{step}$ for the calculated second spectra $S_2(f_2)$ obtained from the time series of the noise integrals $A_j(jT_{step})$. By varying T_{step}, different frequency spans of $S_2(f_2)$ were investigated. Figure 1(b) displays a second spectrum of noise compiled using three different T_{step}'s. A $1/f^\delta$ fit to the second spectrum yields $\delta \simeq 0.8 \pm 0.15$. This agrees quite well with the simulated second spectrum, which supports long-time correlations beyond a collection of two-level systems for which low-frequency $S_2(f_2)$ is white.[36,57]

Figure 1(c) displays the cumulative distribution function of a calculated time series of noise integrals $A_j(jT_{step})$. The distribution has a more pronounced wing at larger noise values than at the beginning of the curve. This asymmetry of wings signifies the non-Gaussian nature of the clustering/declustering induced fluctuations in the simulation. The fitted curve displays lognormal behavior. The lognormal behavior is often observed for processes, which depend on a product of several different probabilities. Then, log of the total probability becomes

normally distributed owing to the law of large numbers.[58] In our simulation, probability of different clusters can be viewed as leading to a product-like probability of the global state.

A scanning electron microscope picture of our graphene Corbino sample with Cr/Au electrodes is illustrated in the bottom left inset of Fig. 2: the size of the disk is 4.5 μm in the outer diameter and 1.8 μm in the inner diameter. The gate voltage dependence of the conductance $G(V_g)$ of our sample (see top right inset of Fig. 2) yielded for the residual charge carrier density $n_0 = 0.1 - 0.4 \times 10^{14} \, m^{-2}$. Details of the sample and its fabrication can be found in Ref. 59. Contact resistance $R_c \sim 500 \, \Omega$ varied slightly depending on the induced strain due to

FIG. 2. Noise power spectral density S_I vs frequency f near the Dirac point at $V_g = -1.20 \, V$ ($n = -1.22 \times 10^{10} \, cm^{-2}$) using a bias voltage corresponding to current $I = 12.9 \, \mu A$. The solid line depicts a fit $1/f^\gamma$ with $\gamma = 1.01$. The bottom left inset displays a false-color scanning electron micrograph of the employed sample. The top right inset displays the gate voltage dependence of the conductance $G(V_g)$.

adsorbed atoms on graphene.[31,59] Mobility of the sample $\sim 10^5$ cm^2/s, most likely limited by hydrocarbon residues.

Figure 2 displays measured current noise power spectral density S_I vs frequency f near Dirac point at $V_g = -1.20$ V using voltage bias corresponding to a current $I \simeq 13\mu$A. Our data can be fit by $S_I(I) = \mathbf{s}\frac{I^\beta}{f^\gamma}$, where $\gamma \simeq 1$, $\beta \simeq 2$, and $\mathbf{s}$ describes the noise magnitude. The noise magnitude $\mathbf{s} = fS_I(I)/I^2 \simeq 2-5 \times 10^{-10}$ is approximately constant and is similar compared with the best low-noise graphene devices.[23,31] As discussed in Ref. 31, the measured $1/f$ noise contains contributions from the contact resistance besides graphene. In this work, we do not consider separation of them but assume that the noise is dominated by graphene near the Dirac point while, at large gate voltage $V_g \geq 40$ V, the noise is dominated by the contact.

We monitored noise at nearly unaltered experimental conditions over long periods of time, typically on the order several hours up to 1 day. We have excluded rare events[60] as we are interested in determining whether the second spectrum is white or colored. A typical record of noise magnitude is illustrated in Fig. 3. The magnitude was determined by fitting the $1/f^\gamma$ spectrum with $\gamma = 1$ to all individual spectra. We also analyzed the statistics of variations in the noise power spectral shape using unconditioned $1/f^\gamma$ fits to the data. These noise exponents as a function of time are displayed as the upper trace in Fig. 3. Non-Gaussian character of the measured graphene noise magnitude is evident already in Fig. 3. The excursions from the mean value are more limited below than above. Hence, the distribution cannot be Gaussian.

Figure 4(a) displays the second spectrum of the measured $1/f$ noise, i.e., power spectral density of the time traces of noise magnitude $\mathbf{s}_j$ illustrated in Fig. 3. Figure 4(a) includes data at $T = 4$ (clean graphene) and 15 K (graphene with adsorbed neon). The second spectra are proportional to $1/f^\delta$, i.e., colored, but no appreciable distinction in the exponent δ is found under the applied different conditions. On average, our experiments yield $\delta = 0.7 \pm 0.3$. The error estimate covers two weighting schemes for the data points: (1) equal weight for all points and (2) same weight for points in each octave [see Fig. 4(a) for the fitted spectra]: the obtained exponents are $\delta = 0.42/0.68$ at 4 K and $\delta = 0.63/0.97$ at 15 K, respectively.

FIG. 3. Noise magnitude $\mathbf{s}(t_j) = \frac{1}{f_1-f_0}\int_{f_0}^{f_1}\frac{f \times S_I(f,t_j)}{I^2}df$ (lower trace, left scale) and exponent γ (upper trace, right scale) of the fits to the measured noise spectra ($f_0 = 1$ Hz and $f_1 = 35$ Hz) in the course of a $\sim$25-h-long measurement at 4 K; an 8 h timescale bar is included.

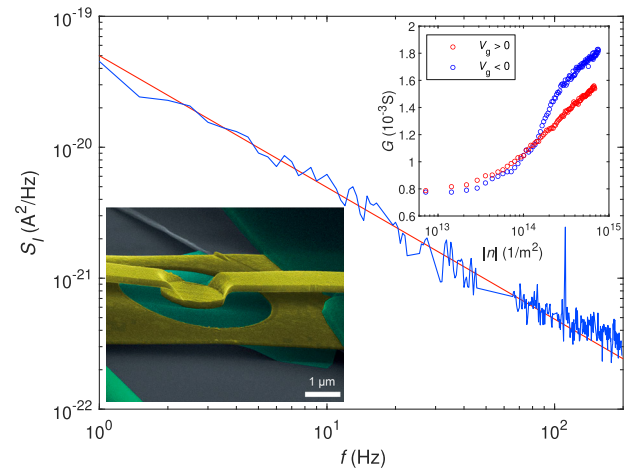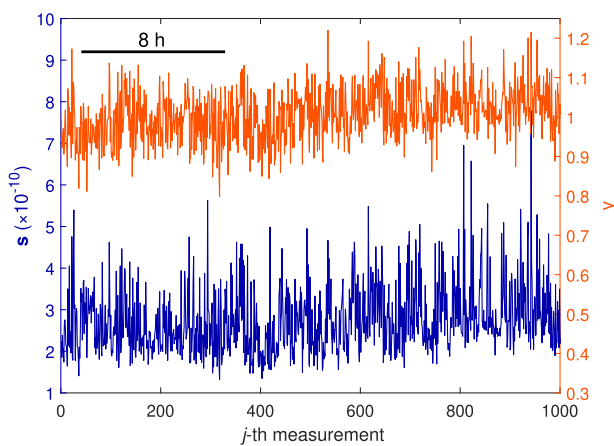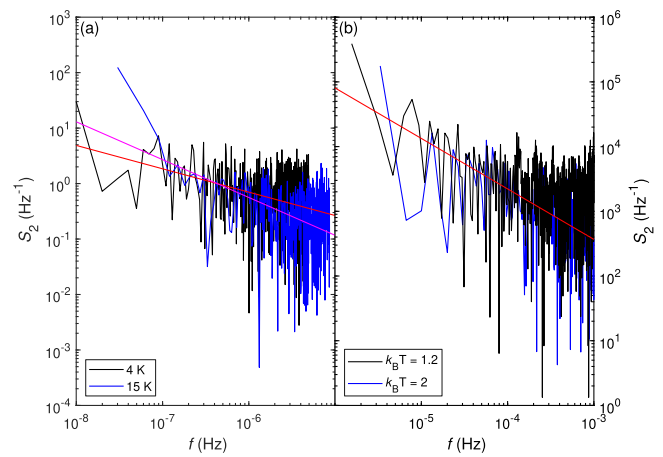**FIG. 4.** (a) Measured, scaled second noise power spectral density S_2 vs frequency f near the Dirac point at $V_g = -1.20$ V ($n = -1.22 \times 10^{10}$ cm^{-2}). The black data trace was measured at 4 K in annealed state while the blue trace was obtained at 15 K with neon adsorbants. The indicated power law fits with $\delta = 0.42/0.68$ at 4 K are obtained using different weighting schemes (see text for details). (b) Simulated, scaled second noise power spectral density S_2 vs frequency f in Corbino geometry obtained for $k_BT = 1.2$ (black) and $k_BT = 2$ (blue) using time series of resistance noise integral $A(t_j) = \int_{f_0}^{f_1} S_R(f, t_j)df$. Red traces are power law fits with $\delta = 0.75$ for both $k_BT = 1.2$ and $k_BT = 2$.

Conclusions of the non-Gaussian character can be quantified from the cumulative distribution functions displayed in Fig. 1(c) for the data at 4 and 15 K. The distributions display a clear, smooth tail toward larger magnitudes. Fitting the distribution, we find quite accurate correspondence with the lognormal distribution, which is illustrated by the dashed–dotted curves. The values of exponents γ determined separately are normally distributed [see the inset in Fig. 1(c)] with a mean of $\langle\gamma\rangle = 1.005$ (0.918) and a standard deviation of $\langle\sigma\rangle = 0.0649$ (0.0578) for data at 4 K (15 K).

Altogether, our kMC simulations turned out to provide an efficient mean to investigate noise phenomena arising due to the dynamics of impurities on 2D materials. Our simulations can be viewed as applicable to various adsorbed atom species in a temperature regime, where the hopping frequency between adjacent lattice sites becomes a few orders of magnitude larger than experimental frequencies. Our simulations indicate presence of long-time correlations, which correspond to a $1/f$ spectrum with upper and lower cutoff frequencies [see Eq. (2)]. This result was found to be valid both for the infinite box and the Corbino disk geometries. For the second spectrum, our simulations yielded $1/f^\delta$ spectrum with an exponent $\delta \simeq 0.8 \pm 0.15$.

Our experiments indicate that the second spectrum of low frequency noise of suspended graphene is colored, with an exponent $\delta \simeq 0.7 \pm 0.3$. This appears to be rather independent of temperature and the amount of weakly absorbed impurities on graphene. The recorded data on $S_I(t)$ displayed strong rare events, which led to irrecoverable level change in the noise magnitude. Unless these events are excluded, the second spectrum would display spectra $1/f^\delta$ with $1 < \delta < 2$. The reason for these jumps remained unclear in the course of our experiments. One option in suspended graphene is flipping of local buckling, which might take place because adsorbed

atoms/molecules induce local strain in the membrane and the distribution of adsorbants varies with time. Consequently, it would be interesting to improve the statistics by performing similar experiments in hBN-encapsulated graphene.

AUTHOR DECLARATIONS
Conflict of Interest

The authors have no conflicts to disclose.

Author Contributions

Weijun Zeng: Data curation (lead); Formal analysis (supporting); Investigation (equal); Methodology (equal); Software (equal); Visualization (equal); Writing – original draft (supporting); Writing – review & editing (supporting). **Kirsi M. Tappura:** Conceptualization (equal); Data curation (equal); Formal analysis (lead); Investigation (equal); Methodology (equal); Software (lead); Visualization (lead); Writing – original draft (supporting); Writing – review & editing (equal). **Masahiro Kamada:** Conceptualization (equal); Data curation (equal); Investigation (equal); Methodology (equal); Software (supporting); Validation (supporting); Visualization (supporting); Writing – review & editing (supporting). **Antti Laitinen:** Investigation (equal); Methodology (equal); Resources (equal). **Heikki Seppä:** Conceptualization (lead); Data curation (supporting); Formal analysis (lead); Funding acquisition (equal); Investigation (equal); Methodology (lead); Supervision (equal); Validation (equal); Visualization (supporting); Writing – original draft (supporting); Writing – review & editing (supporting). **Pertti J. Hakonen:** Conceptualization (lead); Data curation (supporting); Formal analysis (equal); Funding acquisition (lead); Investigation (supporting); Methodology (equal); Project administration (lead); Supervision (lead); Validation (supporting); Visualization (supporting); Writing – original draft (lead); Writing – review & editing (lead).

DATA AVAILABILITY

The data that support the findings of this study are available from the corresponding author upon reasonable request.

REFERENCES

[1]S. Kogan, *Electronic Noise and Fluctuations in Solids*, 1st ed. (Cambridge University Press, New York, NY, USA, 2008).

[2]D. M. Fleetwood, "$1/f$ noise and defects in microelectronic materials and devices," IEEE Trans. Nucl. Sci. **62**, 1462–1486 (2015).

[3]T. Grasser, *Noise in Nanoscale Semiconductor Devices* (Springer International Publishing, Cham, 2020), pp. 1–729.

[4]C. Müller, J. H. Cole, and J. Lisenfeld, "Towards understanding two-level-systems in amorphous solids: Insights from quantum circuits," Rep. Prog. Phys. **82**, 124501 (2019).

[5]H. Wang, C. R. McRae, J. Gao, M. R. Vissers, T. Brecht, A. Dunsworth, D. P. Pappas, and J. Mutus, "Materials loss measurements using superconducting microwave resonators," Rev. Sci. Instrum. **91**, 091101 (2020).

[6]F. N. Hooge, T. G. M. Kleinpenning, and L. K. J. Vandamme, "Experimental studies on $1/f$ noise," Rep. Prog. Phys. **44**, 479–532 (1981).

[7]F. N. Hooge, "$1/f$ noise sources," IEEE Trans. Electron Devices **41**, 1926–1935 (1994).

[8]S. Feng, P. A. Lee, and A. D. Stone, "Sensitivity of the conductance of a disordered metal to the motion of a single atom: Implications for $1/f$ noise," Phys. Rev. Lett. **56**, 1960–1963 (1986).

[9]J. Pelz and J. Clarke, "Quantitative 'local-interference' model for $1/f$ noise in metal films," Phys. Rev. B **36**, 4479–4482 (1987).

[10]J. W. Martin, "The electrical resistivity of some lattice defects in FCC metals observed in radiation damage experiments," J. Phys. F: Met. Phys. **2**, 842–853 (1972).

[11]S. M. K. Nagaev and K. E, "Low-frequency current noise and internal friction in solids," Fiz. Tverd. Tela (Leningrad), Sov. Phys. Solid State **24**, 1921 (1982).

[12]F. Robinson, "A mechanism for 1/f noise in metals," Phys. Lett. A **97**, 162–163 (1983).

[13]N. Giordano, "Defect motion and low frequency noise in disordered metals," Rev. Solid-State Sci. **3**, 27–69 (1989).

[14]H. J. Jensen, "Lattice gas as a model of $1/f$ noise," Phys. Rev. Lett. **64**, 3103–3106 (1990).

[15]N. S. Klonais and J. G. Cottle, "Modeling 1/f noise using a simple physical model based on vacancy motion," MRS Proc. **309**, 321 (1993).

[16]J. Ruseckas, B. Kaulakys, and V. Gontis, "Herding model and $1/f$ noise," Europhys. Lett. **96**, 60007 (2011).

[17]A. A. Balandin, "Low-frequency $1/f$ noise in graphene devices," Nat. Nanotechnol. **8**, 549–555 (2013).

[18]P. Karnatak, T. Paul, S. Islam, and A. Ghosh, "$1/f$ noise in van der Waals materials and hybrids," Adv. Phys. X **2**, 428–449 (2017).

[19]I. Heller, S. Chatoor, J. Männik, M. A. G. Zevenbergen, J. B. Oostinga, A. F. Morpurgo, C. Dekker, and S. G. Lemay, "Charge noise in graphene transistors," Nano Lett. **10**, 1563–1567 (2010).

[20]A. N. Pal, S. Ghatak, V. Kochat, E. S. Sneha, A. Sampathkumar, S. Raghavan, and A. Ghosh, "Microscopic mechanism of $1/f$ noise in graphene: Role of energy band dispersion," ACS Nano **5**, 2075–2081 (2011).

[21]Y. Zhang, E. E. Mendez, and X. Du, "Mobility-dependent low-frequency noise in graphene field-effect transistors," ACS Nano **5**, 8124–8130 (2011).

[22]A. A. Kaverzin, A. S. Mayorov, A. Shytov, and D. W. Horsell, "Impurities as a source of $1/f$ noise in graphene," Phys. Rev. B **85**, 75435 (2012).

[23]M. Kumar, A. Laitinen, D. Cox, and P. J. Hakonen, "Ultra low $1/f$ noise in suspended bilayer graphene," Appl. Phys. Lett. **106**, 263505 (2015).

[24]H. N. Arnold, V. K. Sangwan, S. W. Schmucker, C. D. Cress, K. A. Luck, A. L. Friedman, J. T. Robinson, T. J. Marks, and M. C. Hersam, "Reducing flicker noise in chemical vapor deposition graphene field-effect transistors," Appl. Phys. Lett. **108**, 073108 (2016).

[25]P. Karnatak, T. P. Sai, S. Goswami, S. Ghatak, S. Kaushal, and A. Ghosh, "Current crowding mediated large contact noise in graphene field-effect transistors," Nat. Commun. **7**, 13703 (2016).

[26]B. Pellegrini, "$1/f$ noise in graphene," Eur. Phys. J. B **86**, 373 (2013).

[27]J. Lu, J. Pan, S. S. Yeh, H. Zhang, Y. Zheng, Q. Chen, Z. Wang, B. Zhang, J. J. Lin, and P. Sheng, "Negative correlation between charge carrier density and mobility fluctuations in graphene," Phys. Rev. B **90**, 085434 (2014).

[28]P. Dutta and P. M. Horn, "Low-frequency fluctuations in solids: $\frac{1}{f}$ noise," Rev. Mod. Phys. **53**, 497–516 (1981).

[29]A. Rehman, J. A. Delgado Notario, J. Salvador Sanchez, Y. M. Meziani, G. Cywiński, W. Knap, A. A. Balandin, M. Levinshtein, and S. Rumyantsev, "Nature of the $1/f$ noise in graphene-direct evidence for the mobility fluctuation mechanism," Nanoscale **14**, 7242–7249 (2022).

[30]M. Kamada, W. Zeng, A. Laitinen, J. Sarkar, S.-S. Yeh, K. Tappura, H. Seppä, and P. Hakonen, "Suppression of $1/f$ noise in graphene due to non-scalar mobility fluctuations induced by impurity motion," arXiv:2112.11933 (2021).

[31]M. Kamada, A. Laitinen, W. Zeng, M. Will, J. Sarkar, K. Tappura, H. Seppä, and P. Hakonen, "Electrical low-frequency $1/f^{\gamma}$ noise due to surface diffusion of scatterers on an ultra-low-noise graphene platform," Nano Lett. **21**, 7637–7643 (2021). https://doi.org/10.1021/acs.nanoLetters1c02325.

[32]K. S. Ralls, W. J. Skocpol, L. D. Jackel, R. E. Howard, L. A. Fetter, R. W. Epworth, and D. M. Tennant, "Discrete resistance switching in submicrometer silicon inversion layers: Individual interface traps and low-frequency ($1/f$) noise," Phys. Rev. Lett. **52**, 228–231 (1984).

[33]K. S. Ralls and R. A. Buhrman, "Defect interactions and noise in metallic nano-constrictions," Phys. Rev. Lett. **60**, 2434–2437 (1988).

[34]P. J. Restle, R. J. Hamilton, M. B. Weissman, and M. S. Love, "Non-Gaussian effects in $1/f$ noise in small silicon-on-sapphire resistors," Phys. Rev. B **31**, 2254–2262 (1985).

[35]G. A. Garfunkel, G. B. Alers, and M. B. Weissman, "Mesoscopic noise studies of atomic motions in cold amorphous conductors," Phys. Rev. B **41**, 4901–4919 (1990).

[36]M. B. Weissman, "What is a spin glass? A glimpse via mesoscopic noise," Rev. Mod. Phys. **65**, 829–839 (1993).

[37]G. T. Seidler and S. A. Solin, "Non-Gaussian $1/f$ noise: Experimental optimization and separation of high-order amplitude and phase correlations," Phys. Rev. B **53**, 9753–9759 (1996).

[38]K. M. Abkemeier, "Weakly non-Gaussian processes in a-Si:H conductance noise," Phys. Rev. B **55**, 7005–7013 (1997).

[39]J. Jaroszyński, D. Popović, and T. M. Klapwijk, "Universal behavior of the resistance noise across the metal-insulator transition in silicon inversion layers," Phys. Rev. Lett. **89**, 276401 (2002).

[40]C. C. Yu, "Why study noise due to two level systems: A suggestion for experimentalists," J. Low Temp. Phys. **137**, 251–265 (2004).

[41]V. Orlyanchik, V. I. Kozub, and Z. Ovadyahu, "Non-Gaussian conductance noise in disordered electronic systems due to a nonlinear mechanism," Phys. Rev. B **74**, 235206 (2006).

[42]P. V. Lin, X. Shi, J. Jaroszynski, and D. Popović, "Conductance noise in an out-of-equilibrium two-dimensional electron system," Phys. Rev. B **86**, 155135 (2012).

[43]N. Ubbelohde, C. Fricke, C. Flindt, F. Hohls, and R. J. Haug, "Measurement of finite-frequency current statistics in a single-electron transistor," Nat. Commun. **3**, 612 (2012).

[44]F. M. D. Pellegrino, G. Falci, and E. Paladino, "Second spectrum of charge carrier density fluctuations in graphene due to trapping/detrapping processes," arXiv:2305.07628 (2023).

[45]In the Corbino-geometry simulation, part of the noise arises from the diffusing impurities sticking to the boundary. Only in the infinite box simulation, the contact noise due to particles at the edges can be avoided. In this work, we do not try to separate contact noise from graphene noise. The data we provide are measured at the Dirac point where the role of the contact noise is the smallest and it can be neglected.

[46]J. Moser, A. Barreiro, and A. Bachtold, "Current-induced cleaning of graphene," Appl. Phys. Lett. **91**, 163513 (2007).

[47]F. Hooge, "Discussion of recent experiments on $1/f$ noise," Physica **60**, 130–144 (1972).

[48]D. M. Fleetwood and N. Giordano, "Direct link between $1/f$ noise and defects in metal films," Phys. Rev. B **31**, 1157–1160 (1985).

[49]S. J. Plimpton, C. C. Battaile, M. E. Chandross, E. A. Holm, A. P. Thompson, V. Tikare, G. J. Wagner, E. B. Webb III, X. W. Zhou, C. G. Cardona, and A. Slepoy, "Crossing the mesoscale no-mans land via parallel kinetic Monte Carlo," Technical Report SAND2009-6226.

[50]S. Plimpton, A. Thompson, and A. Slepoy, "https://spparks.sandia.gov/," 2021.

[51]W. E. Carlos and M. W. Cole, "Interaction between a He atom and a graphite surface," Surf. Sci. **91**, 339–357 (1980).

[52]M. W. Cole, D. R. Frankl, and D. L. Goodstein, "Probing the helium-graphite interaction," Rev. Mod. Phys. **53**, 199–210 (1981).

[53]J. V. Barth, "Transport of adsorbates at metal surfaces: from thermal migration to hot precursors," Surf. Sci. Rep. **40**, 75–149 (2000).

[54]S. M. Gatica and M. W. Cole, "To wet or not to wet: That is the question," J. Low Temp. Phys. **157**, 111–136 (2009).

[55]In the infinite box geometry, we note that the stable configuration of impurities would be one single cluster (this corresponds to gas–liquid phase transition). The large cluster would then become the source of emitted free particles driven by thermal activation. However, the time scales and $E_d/k_B T$ values employed in our simulations (up to 10^9 steps of Monte Carlo modified configurations) did not lead to substantial global clustering of the impurities.

[56]COMSOL multiphysics [textregistered], 2021.

[57]M. B. Weissman, Rev. Mod. Phys. **60**, 537 (1988).

[58]E. W. Montroll and M. F. Shlesinger, "On $1/f$ noise and other distributions with long tails," Proc. Natl. Acad. Sci. U. S. A. **79**, 3380–3383 (1982).

[59]M. Kumar, A. Laitinen, and P. Hakonen, "Unconventional fractional quantum Hall states and Wigner crystallization in suspended Corbino graphene," Nat. Commun. **9**, 2776 (2018).

[60]All these extensive records seem to have large jumps in the magnitude of the noise. If such rare jump events (about once per day) in the noise are included, the second spectrum becomes proportional to $1/f^2$.